International Journal of Science and Research Archive
eISSN: 2582-8185
Cross Ref DOI: 10.30574/ijsra
Journal homepage: https://ijsra.net/

(RESEARCH ARTICLE)

Check for updates

# Effects of Deep Beam Characteristics on Ultimate Load Capacity, Failure Mode, and Serviceability Performance of Reinforced Concrete Deep Beams

Oluwaseun Samuel Oguntoye *, Lekan Makanjuola Olanitori, Catherine Mayowa Ikumapayi, and Samuel Lambe Akingbonmire

*Department of Civil Engineering, School of Infrastructure, Minerals and Manufacturing Engineering, The Federal University of Technology Akure, Nigeria.*

International Journal of Science and Research Archive, 2026, 20(01), 763–775

Publication history: Received on 14 June 2026; revised on 19 July 2026; accepted on 22 July 2026

Article DOI: https://doi.org/10.30574/ijsra.2026.20.1.1521

## Abstract

Deep beams are reinforced concrete structural members characterized by a small span-to-depth ratio, in which loads are transferred primarily through arching action rather than conventional flexural behaviour. This study experimentally investigated the influence of deep beam characteristics on structural performance under a centrally applied point load. Four reinforced concrete deep beam specimens with varying effective span-to-depth depth ($L_e/h$) and shear span-to-depth ((a/d)) ratios were tested to failure using a 300 kN Universal Testing Machine (UTM). The experimental programme evaluated the first crack load, ultimate load capacity, midspan deflection, final flexural crack width, and observed failure mode. The results showed that decreasing the ($L_e/h$) ratio from 2.5 to 1.7 and the (a/d) ratio from 1.4 to 0.9 significantly enhanced structural performance. The first crack load increased from 89.97 kN to 180.79 kN, while the ultimate failure load increased from 124.51 kN to 241.43 kN. Deflection decreased from 0.21 mm to 0.08 mm, indicating increased stiffness, whereas the final crack width increased from 2.54 mm to 3.58 mm due to the higher stress levels sustained before failure. All beam specimens exhibited diagonal cracking followed by shear-compression failure, confirming that shear behaviour governed the ultimate response. The study concludes that reducing the effective span-to-depth and shear span-to-depth ratios significantly improves the strength and stiffness of reinforced concrete deep beams through enhanced arching action. Lower ($L_e/h$) and (a/d) ratios are therefore recommended for heavily loaded deep beams, with adequate reinforcement detailing to control crack widths and ensure satisfactory serviceability.

**Keywords:** Deep Beams; Span-to-depth ratio; Shear span-to-depth ratio; Ultimate load capacity; Deflection; Crack width; Failure mode

## 1. Introduction

Deep beams are structural elements loaded as simple beams in which a significant amount of the load is carried to the supports by a compression force combining both the load and the reaction. As a result, the strain distribution is no longer considered linear, and the shear deformations become significant when compared to pure flexure [1]. Deep beams are structural members characterized by a large depth relative to their span [2,3,4,5].

Reinforced concrete deep beams are mainly used in massive application in various civil engineering structures, such as transfer girders in tall buildings, offshore structures, shear walls, wall footings, foundation pile caps and bridges [6]. The strain distribution in deep beams is not linear across the transverse section as in the elementary beam theory. It is because that the transfer of load is happening mainly through the arch action [7] So, the traditional beam theory cannot be used for deep beams [6].

* Corresponding author: Oluwaseun Samuel Oguntoye

These structural elements belong to D (disturbed) regions, which have traditionally been designed using empirical formulae or using past experience. Strut and tie method (STM) offers an alternative to such empirical method [8]. Designing deep beams to resist shear force has been a massive challenge because they are more prone to shear failures arising from shear stress accumulation in the span. Proper understanding of shear stress characteristics can assist in providing safer design and prevent failure in deep beams which consequently lead to saving lives and properties, shear stress is the major cause of failure in deep beam [9].

The structural design standards, [10] and [7], adopted the use of strut-and-tie modelling (STM) for the strength design of deep beams or other regions of discontinuity in 1994 and 2002, respectively [11]. The Strut-and-Tie Method (STM), which models load transfer through compression struts, tension ties, and nodal zones [12,13,14,15], provides the design engineers a more flexible and easier design procedure for the design of the beam.

There are different definitions of deep beam by different codes of practice. For example, Egyptian Code (ECCS) defines the deep beam as a beam with $^{L_e}/_h < 2.0$, American Code

(ACI 318 – 2008) as $^{L_e}/_h < 4.0$, Canadian Code (CAN3-A23.3-M84) as $^{L_e}/_h < 1.25$, Euro Code 2 (BS EN 1992-1-1:2004) as, $^{L_e}/_h < 3.0$; CIRIA manual as $^{L_e}/_h < 2$, and Indian Standard as $^{L_e}/_h < 2$, where $L_e$ is the effective beam span and $h$ is the overall depth of the beam respectively. Hence, the focus of this research is to verify the applicability of the recommendations of the ACI - 318 (2008) code, using STM in the analysis, design and construction of deep beams using locally sourced materials in Nigeria.

Construction aggregate, or simply 'aggregate', is a broad category of particulate materials used in construction which includes sand (fine aggregate), and granite (coarse aggregates). One of the most critical factors influencing deep beam performance is the quality of fine aggregates (sand) used in concrete production. Sand contributes to the packing density, workability, and strength of concrete [16].

This research focuses on the experimental flexural test on four different types of deep beams which confirmed that the strength of deep beams depends mainly on several characteristics such as shear span to effective depth ratio (a/d), beam span to depth ratio ($L_e$/h), and their effect on deflection, flexural crack width, and how they affect the strength of the deep beams.

### 1.1. Statement of the problem

The statement of the problem in this experimental flexural test addresses the limitations of classical beam theory in predicting the complex, non-linear stress distribution and failure modes of deep beams. Specifically, classical Bernoulli-Euler theories fail to accurately account for the pronounced effects of low span-to-depth ratios and shear span-to-depth ratios on ultimate load capacity, flexural deflection, and crack width [17,18]

### 1.2. Justification of the Experiment

The experiment is justified for the following practical and theoretical reasons:

Inadequate code provisions in standard building codes such as ACI or Eurocode have varying and sometimes conservative shear provisions for deep beams which typically characterized by an le/h < 4.0 and a/d < 2.0. The experimental test verifies how the deep beams variations align with design guidelines.

Load path analysis under point loading, for deep beams rely on arching action and a two-dimensional stress distribution rather than simple bending. The experiment isolates how changing geometries shift the failure mechanism from pure flexure to brittle shear.

Serviceability evaluation of deep beams by using a UTM to detect ultimate loads and mapping crack propagation, structural engineers can better predict flexural deflection and control crack width, both of which dictate a structure's long-term integrity.

### 1.3. Objective of the study

To investigate the effect of span-to-depth ($L_e/h$) and shear span-to-depth (a/d) ratios on the ultimate load capacity, failure mechanisms, and serviceability performance of deep reinforced concrete beams under a single point load.

## 2. Literature Review

### 2.1. Preamble

Structures in civil engineering consist of various components and elements which includes foundations, columns, beams, slabs etc. They are typically designed to withstand various loads they are meant to carry [19]. Failure sometimes is inevitable and can occur in one or more of these structural components. Hence, structural elements taking for instance reinforced concrete beams which span horizontally and transfer load from slab to the column usually need to be strengthened [20].

### 2.2. Concrete as a construction material

An important structural material in civil engineering construction is concrete. Concrete is a composite material mainly consisting of aggregates of different sizes embedded in mortar matrix. The mortar matrix has high porosity, and the pores are filled with air and water. A large number of bond micro-cracks exist at the interface between the coarse aggregates and the matrix. These properties strongly affect the complex nonlinear behavior of concrete [21]. Concrete is widely used in various building structures, which plays a very important role in the stability of the building structure and concrete itself has the irreplaceable advantages of other building materials [22]. The composite materials of concrete are cement, sand, gravel, and water, sometimes mixed with a small quantity of various additives. These raw materials are successively mixed, cast, compacted, and cured, and gradually coagulated and hardened and, then, concrete is made. The main reason for concrete having complicated behavior is that concrete is a multiphase material of inhomogeneous and anisotropic and is varied with time and environmental conditions, as shown by the existing experimental investigation [23].

### 2.3. Deep Beams as a Structural Member

Deep beams are structural members with a relatively large depth compared to their span [24,4]. They are widely used in civil engineering applications such as bridges, transfer girders, and foundation beams. Their behaviour has been extensively studied to develop reliable design methods [25]. Common failure modes include strut crushing, diagonal splitting, and shear-compression failure, as illustrated in Figure 1. Researchers have extensively studied the behavior of deep beams to develop effective design approaches and guidelines [25].

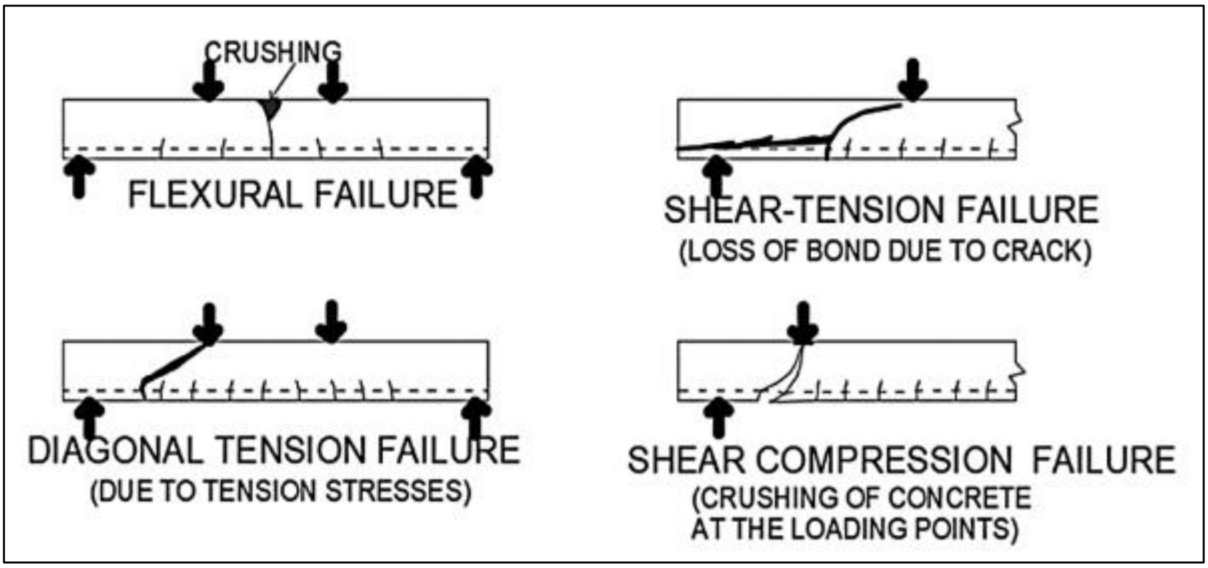


**Figure 1** Failure Points in Deep Beams [26]

### 2.4. Role of Fine Aggregates in Concrete

The quality of sand is crucial to how deep beams perform. It dictates the concrete's workability, packing density, and strength. Furthermore, inconsistencies in sand's particle size, mineral makeup, or thermal stability can drastically change how a beam behaves under normal loads or extreme conditions like fire. Fine aggregates, typically sand (< 5mm), are vital in concrete, comprising 35-45% of the total volume to fill voids between coarse aggregates, increasing mix density. Their grading, shape, and mineral composition affect workability, density, and strength. [27] highlighted that well graded sands improve packing density, reducing voids and enhancing compressive strength. Sands with excessive fines (clay and silt) can impair bonding and increase shrinkage. Thus, characterization of sand is vital for predicting concrete performance. They improve workability, act as fillers, reduce porosity, and ensure a smooth surface finish. Properly graded fine aggregates minimize voids and increase the overall compressive strength. Fine aggregates function to fill the pores between coarse aggregates to minimize the air content in the concrete mixture so as not to reduce the strength of concrete due to the gradation and uniformity of the aggregate [16].

## 3. Materials and Methods

### 3.1. Materials

The materials used for this study were Ordinary Portland cement of grade 32.5 (binder), sand (fine aggregate), crushed granite (coarse aggregate), high yield reinforcement bars, and potable water. The concrete grade is C20/25, while the yield stress for the reinforcement bar is 410 $N/mm^2$.

### 3.2. Equipment and Instrumentation

The major equipment and instrumentation used for testing the cube and beam specimens prepared for this study include: (i) Universal Testing Machine, (ii) Avongard standard tell-tale crack monitor, (iii) Linear Variable Displacement Transducer (LVDT) or dial gauges, and (iv) strain gauges. The UTM is shown in Figure 2.

**Figure 2** Universal Testing Machine

### 3.3. Experimental Programme

#### *3.3.1. Mix design*

The concrete mix was designed using the British Standard (BS) method, which defines the required performance while allowing the producer to determine mix proportions, subject to a minimum cement content [28]. Mix proportioning entails selecting optimal ratios of cement, fine and coarse aggregates, and water to achieve specified properties. The target mean compressive strength at 28 days is established based on the characteristic strength and the site's quality control level. Because of material variability, the mix is designed for a higher mean strength than specified; this statistical increase is known as the "margin."

### *3.3.2. Deep beams preparation*

The deep beams in this study were prepared after mechanical properties of concrete samples were determined based on the strut and tie method developed by American concrete institute [6]. The concrete prescribed mix used gives compressive strength of concrete cube to be 20.29 N/mm$^2$ at 28 days. A total of four deep beams specimen with varying sizes were prepared and cast. The beams cast were prepared accordingly using the result gotten from the concrete prescribed mix. The fine aggregate, coarse aggregate, cement and water were batched in ratio 1:1.5:3, mixed thoroughly until a uniform mix was achieved. The prepared reinforcements were then placed into the already made formwork, and the concrete was placed into the formwork in layers. The placed concrete was properly compacted using the needle vibrator to ensure that there was no void in the concrete beam's specimens. The beams specimens were removed after 24 hours from the moulds and gunnysacks were used to cover beams and water was sprinkled over the beams at every 4 hours interval to avoid evaporation of moisture from their surfaces, in order to ensure full compressive strength after 28 days curing, before they were transported to the laboratory, where flexural tests were conducted on the beam's specimens.

### *3.3.3. Beam specimen details*

The study evaluated 4 simply supported deep beams of varying cross sections but the position and numbers of the reinforcement bars were fixed. Each beam sample had a length of 1000 mm of rectangular cross section. The flexural reinforcement consisted of 2Y10 mm deformed steel bars, which were placed at the bottom of the beam cross section, 2Y10 mm as compression reinforcement placed at the top of cross section and Y8 mm as shear reinforcement at spacing of 100 mm each. All specimens were prepared under controlled conditions in the Civil Engineering Department at The Federal University of Technology, Akure (FUTA). Beam dimensions and cross sections are detailed in Table1. Therefore, the beams prepared for this work were simply supported deep beams with effective span to effective depth $^{L_e}/_{d}$ ratios of 2.5, 2.2, 1.9 and 1.7 and shear span to effective depth ($^{a}/_{d}$) ratios of 1.4, 1.3, 1.1 and 0.9 respectively, which are within the ACI 318-2008 Clause 10.7.1 provisions. with their design adhering to standards.

**Table 1** Experimental Beams Details

| Beam No | Longitudinal Section | Cross Section |
|---|---|---|
| B1 | 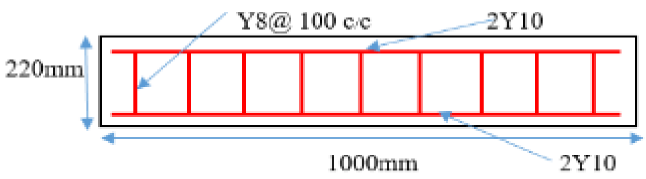  | 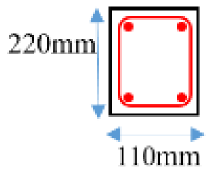  |
| B2 | 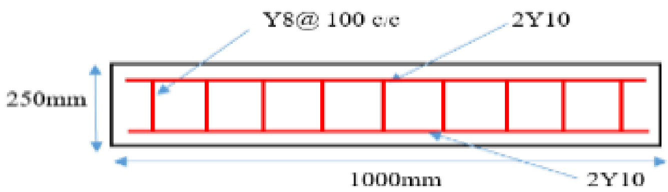  | 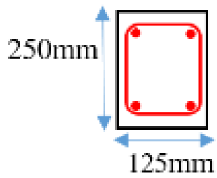  |
| B3 | 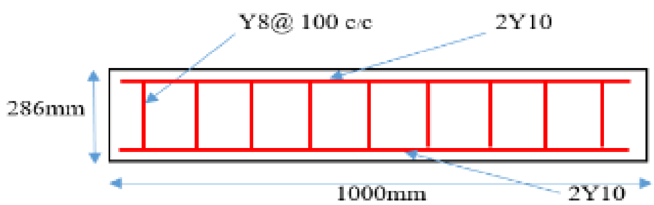  | 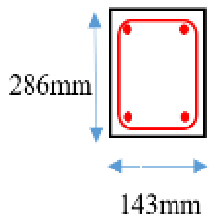  |

| | | |
|---|---|---|
| B4 | 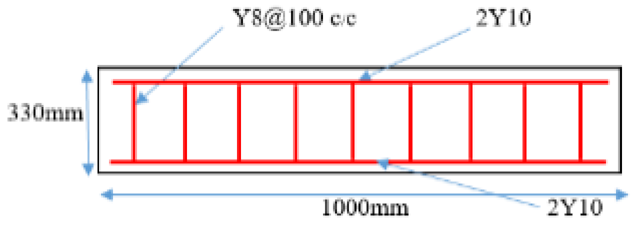  | 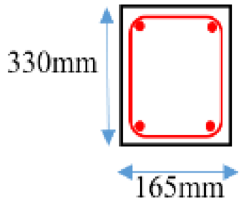  |

### 3.4. Loading of beam specimen for flexural strength test

The beams were loaded with a point load, applied at the center of the beam with effective length of 550 mm. The beams were subjected to flexural test till failure under a point load as shown in plate 3 to 10. The loading was applied in form of a point load at the mid span of the beam with a controlled loading rate up to failure. The tests were carried out on the universal testing machine (UTM) having maximum capacity of 300 kN. Initial cracking load, ultimate load, crack width, and crack development at the D region of the deep beams surface were recorded using an Avogadro strain gauge with ±10 mm resolution. Additionally, load–deflection behaviour, failure modes, and crack pattern were determined. The deflection of the beams is calculated using Equation 1.

$$\partial = \frac{FL^3}{48EI} \qquad (1)$$

Where;
F is the load at the collapsed point,
L is the effective length of the support span,
E is the young modulus,
I is the moment of inertia and
***∂*** is the deflection.

Moment of inertia formula is shown in Equation 2.

$$I = \frac{bh^3}{12} \qquad (2)$$

Where;
b is the width of the beam; and
h is the height of the beam

$$E = 5000(fk)^{0.5} \qquad (3)$$

Where, $f_k$ is the concrete compressive strength

## 4. Results and discussion

The results of the tests carried out on the experimental beams are presented in the sections below.

### 4.1. The Results of Tests on the Beams

These results of the tests carried out on the beams are presented in Table 2.

**Table 2** Experimental loads at first crack, collapsed, and span depth ratio

| **Type** | **Load at First Crack (kN)** | **Exp. Load $P_{AUL}$ (kN)** | $L_e$ **(mm)** | **b (mm)** | **h (mm)** | $L_e/h$ | **Reinforcement** |
|---|---|---|---|---|---|---|---|
| $B1_{110\times220}$ | 89.97 | 124.51 | 550 | 110 | 220 | 2.5 | 2Y10 T &B |
| $B2_{125\times250}$ | 121.09 | 162.13 | 550 | 125 | 250 | 2.2 | 2Y10 T &B |
| $B3_{143\times286}$ | 142.97 | 192.43 | 550 | 143 | 286 | 1.9 | 2Y10 T &B |
| $B4_{165\times330}$ | 180.79 | 241.43 | 550 | 165 | 330 | 1.7 | 2Y10 T &B |

The provided experimental data from Table 2 shows that as the shear span-to-depth ratio $L_e/h$ decreases from 2.5 to 1.7, both the cracking load and ultimate load capacity of the beams significantly increase, demonstrating the dominance of arch action over traditional slender beam behavior in deeper sections. The load at first crack increases proportionally as the beam dimensions (width b and effective depth d) increase. Beam B1 (110 × 220 mm) cracks at 89.97 kN, while Beam B4 (165 × 330 mm) withstands 180.79 kN before cracking. This indicates that larger cross-sectional areas provide higher tensile resistance before yielding. The ultimate load capacity follows a similar upward trajectory. Beam B1 fails at 124.51 kN, whereas B4 reaches 241.43 kN. The ratio of reserve strength (Ultimate Load ÷ Cracking Load) ranges between 1.34 and 1.38 across all four beam types. This implies that the post-cracking reserve capacity remains relatively stable, regardless of the beam dimensions, and is supported by the identical longitudinal reinforcement (2Y10 top and bottom). The shear span-to-depth ratio $L_e/h$ decreases from 2.5 in Beam B1 to 1.7 in Beam B4. As this ratio decreases, both the ultimate load and cracking load increase. Because the shear span ($L_e$ = 550\) mm) remains constant across all tests, beams with smaller overall depths (h) exhibit larger ratios. Beams with lower ratios (like B4 at $L_e/h$ = 1.7) transition from slender beam behavior (governed by diagonal tension) to arch action. This mechanism allows the load to be transferred directly to the supports via a concrete compression strut, resulting in a substantially higher ultimate load capacity.

### 4.2. Beams Cracking Behavior and Failure Mode Observations

The cracking behavior and failure mode of all the deep beams under loading was observed since few concepts had been taken into consideration as the basis of reinforced concrete deep beam shear failure mode and according to these concepts once inclined cracking was initiated to propagate, the reinforced concrete deep beam with shear reinforcement acted like a truss with concrete between two alternative inclined cracks and shear reinforcement acted like strut and tie respectively [29]. It has seven common types of failure, which are shear compression failure, inclined compression failure, inclined tension failure, direct-shear failure, extrusion failure, bending-shear failure and bending failure. In this experiment during the loading, the failure mode of all the specimens was shear-compression failure. The common mode of failure of deep beams is shear compression failure. In Figure 3, a representative pattern of cracking is presented. This form of failure mode is identified by flexural cracks located in the tension surface in the middle of the span that was followed by development of inclined cracks. Since the inclined cracks spread in the direction of the loading point, the concrete crushing takes place in the upper end part of the inclined crack at the ultimate stage of failure. This was predictable given that earlier studies had the same finding.

**Figure 3** Crack pattern at failure for $Beam_{165\times330}$

### 4.3. Crack Width of Experimental Beams

A special gauge that is capable of measuring the crack width of the experimental beams at various locations at an accuracy of 0.01 mm was used in the measurements. The loads that were associated to the appearance and progress of cracks at various stages of loading were recorded. The cracks (i.e., inclined) were initially observed in the middle of the depth of the beams and then proceeded towards the load and support plates. The further load added increased and prolonged the already existing diagonal cracks thus introducing new diagonal cracks. The cracks hardly penetrated half-way through the beam's sections but all the diagonal cracks noticeably extended and were enlarged long as the ultimate collapse of the beams took place. The reinforced concrete deep beams were also subjected to maximum crack widths of the diagonals at the initial load and the failure load. Table 3 indicates the maximum width of diagonal cracks in deep beam of reinforced concrete under various loads that are applied and also a/d.


**Figure 4** 110 x 220 mm Deep Beam before loading


**Figure 5** 110 x 220 mm Deep Beam After loading to failure


**Figure 6** 125 x 250 mm Deep before loading


**Figure 7** 125 x 250 mm Deep Beam after loading to failure


**Figure 8** 143 x 286 mm Deep Beam before loading


**Figure 9** 143 x 286 mm Deep Beam after loading to failure

|  |  |
|---|---|
| **Figure 10** 165 x 330 mm Deep Beam before loading | **Figure 11** 165 x 330 mm Deep Beam After loading to failure |

**Table 3** Maximum crack width of the experimental beams at initial and failure loads

| Beam No | a/d Ratio | Initial flexural load (kN) | Initial crack width (mm) | Failure Load (kN) | Final crack width (mm) |
|---|---|---|---|---|---|
| $B1_{110 \times 220}$ | 1.4 | 89.97 | 0.65 | 124.51 | 2.54 |
| $B2_{125\times250}$ | 1.3 | 121.09 | 0.85 | 162.13 | 2.87 |
| $B3_{143\times286}$ | 1.1 | 142.97 | 0.91 | 192.43 | 3.16 |
| $B4_{165\times330}$ | 0.9 | 180.79 | 1.01 | 241.43 | 3.58 |

Based on the Table 3, results, it is apparent that, the lower the a/d ratio, the larger the maximum width (w) of diagonal crack that was measured in each of the steps of the load increment. The width of the cracking of $B1_{110 \text{ x } 220}$ at 89.97 kN (Initial load) measured around 0.65 mm. The width of the crack increased with time of loading to about 0.65 to 2.54 mm when the loading reached 124.51 kN (failure load). The cracks were seen to open at an early stage in the loading process in $B2_{125\text{x}250}$, and the crack width was about 0.85mm at a load of 121.09 kN. On adding load, the width of the crack began expanding at a high rate up to 2.87 mm at 162.13 kN. $B3_{143\text{x}286}$ failed with shear at first 142.97 kN, maximum shear width 0.91 mm and subsequently, at 192.43 kN, it failed with shear and maximum shear width is 3.16 mm. The other beams were not different as $B4_{165\text{x}330}$ increased the maximum width of the crack of 1.01 mm at 180.79 kN up to 3.58 mm at 241.43 kN.

### 4.4. Experimental Beams Deflection

The results of experimental flexural test on four types of deep beams at collapsed or failure loads and the maximum deflections are shown in Table 4.

**Table 4** Maximum deflection of the experimental beams at failure loads

| Beam ID | Shear Spacing (mm) | Failure load (kN) | b (mm) | h (mm) | $L_e$ (mm) | a/d Ratio | Deflection (mm) |
|---|---|---|---|---|---|---|---|
| 110 x 220 | 100 | 124.51 | 110 | 220 | 550 | 1.4 | 0.21 |
| 125 x 250 | 100 | 162.13 | 125 | 250 | 550 | 1.3 | 0.17 |
| 143 x 286 | 100 | 192.43 | 143 | 286 | 550 | 1.1 | 0.12 |
| 165 x 330 | 100 | 241.43 | 165 | 330 | 550 | 0.9 | 0.08 |

Based on the provided dataset, the analysis reveals that increasing the beam cross-sectional dimensions (b × h) leads to a higher failure load capacity and a significant reduction in maximum deflection at failure, even when the clear span ($L_e$) and stirrup shear spacing remain perfectly constant at 550 mm and 100 mm respectively. Failure load enhancement shows that beam size expands from 110 × 220 mm to 165 × 330 mm, the ultimate carrying capacity jumps from 124.51 kN to 241.43 kN (a 93.9 % increase). Despite carrying nearly double the load, the largest beam experiences the least deformation. Ultimate deflection drops steeply from 0.21mm to 0.08 mm (a 61.9 % decrease). The a/d ratio drops systematically from 1.4 down to 0.9 as the overall cross-sectional depth (h) grows.

**Table 5** Summary of characteristics of deep beams on ultimate load, deflection, and flexural crack width,

| **Beam No** | $L_e/h$ | **a/d Ratio** | **Load at First Crack (kN)** | **Failure Load (kN)** | **Deflection (mm)** | **Final crack width (mm)** |
|---|---|---|---|---|---|---|
| B1$_{110 \times 220}$ | 2.5 | 1.4 | 89.97 | 124.51 | 0.21 | 2.54 |
| B2$_{125 \times 250}$ | 2.2 | 1.3 | 121.09 | 162.13 | 0.17 | 2.87 |
| B3$_{143 \times 286}$ | 1.9 | 1.1 | 142.97 | 192.43 | 0.12 | 3.16 |
| B4$_{165 \times 330}$ | 1.7 | 0.9 | 180.79 | 241.43 | 0.08 | 3.58 |

The data demonstrates the classic behavior of deep beams dominated by strut-and-tie action rather than conventional sectional flexure. As the effective span-to-depth ratio ($L_e/h$ ) and shear span-to-depth ratio (a/d) decrease, the beam behavior transitions from shallow beam bending to deep beam arch action. There is a clear inverse relationship between the geometrical ratios ($L_e/h$ , a/d) and the load-carrying capacity. As ($L_e/h$) decreases from 2.5 to 1.7 and a/d decreases from 1.4 to 0.9, the ultimate failure load increases substantially from 124.51 kN (B1) to 241.43 kN (B4). It is also critical to note that as the ratios decrease, the cross-sectional dimensions increase (from 110 × 220 mm to 165 × 330 mm). This increased cross-sectional area provides a larger concrete compressive zone, further boosting both cracking and ultimate strength. The reserve strength (the margin between first crack and failure load) remains highly significant across all beams, confirming that deep beams do not fail immediately upon cracking due to internal force redistribution. The effect of deep beam characteristics on serviceability limit state (deflection) shows as ($L_e/h$ ) decreases from 2.5 to 1.7, the maximum deflection drops drastically from 0.21 mm (B1) to 0.08 mm (B4), which increased beam stiffness. A lower ($L_e/h$ ) implies a much deeper beam relative to its span. The moment of inertia ($I = bh^3/12$) increases cubically with depth, creating an exceptionally stiff member that experiences negligible mid-span deflection under high ultimate loads. The final crack width represents another critical serviceability limit state, governing durability and corrosion protection. Unlike deflection, the final crack width increases as the geometrical ratios decrease, moving from 2.54 mm (B1) to 3.58 mm (B4). Because beam B4 fails at a much higher load (241.43 kN) compared to B1 (124.51 kN), it stores significantly more strain energy prior to failure. When failure occurs, this massive energy release manifests as wider, more severe macro-cracks. Finally, the deep beams with low a/d ratios, failure is often governed by the splitting of the concrete compressive strut due to transverse tensile stresses. These tensile stresses run perpendicular to the line of the strut. As the load maximizes, these internal splitting cracks open up drastically, resulting in a larger final crack width at the ultimate limit state [30].

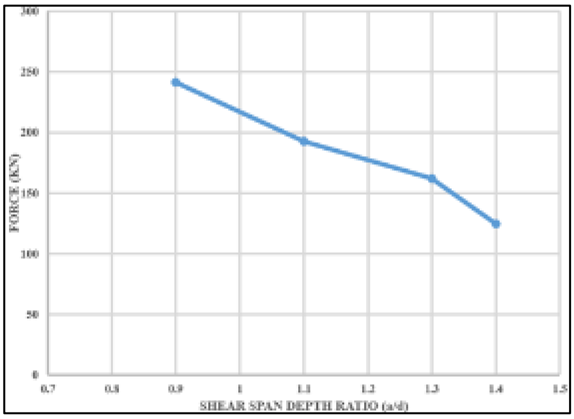


**Figure 12** Effect a/d ratio on the ultimate loads of the beams

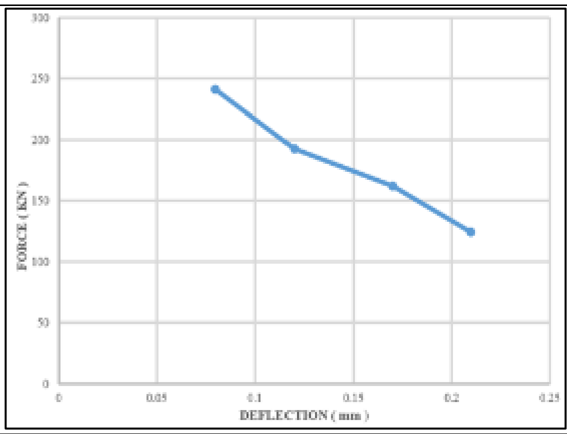


**Figure 13** Load - deflection Relationship

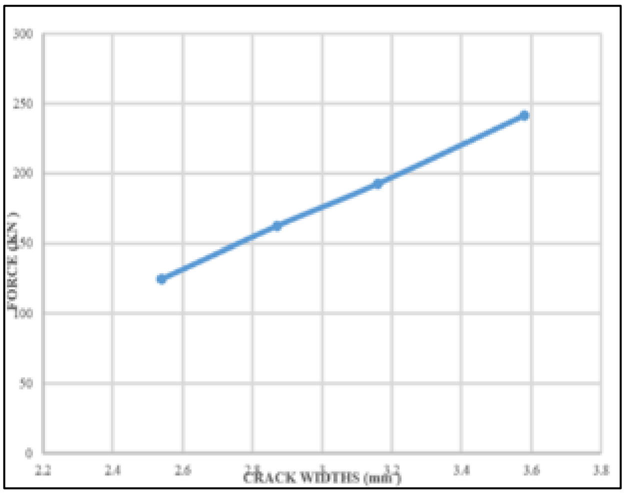


**Figure 14** Load crack width plot for beams at failure

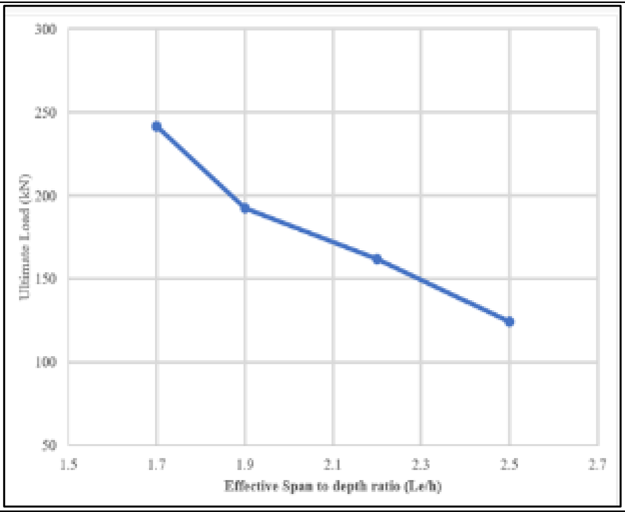


**Figure 15** Effect $L_e/h$ ratio on the ultimate loads of the beams

Figure 12 shows the plot of the experimental collapsed load against the shear span depth ratio of the beams. It could be seen from the graph how both parameters Force P and Shear span depth ratio a/d show that, as the ultimate load on beams experimented on decreases on the chart, the shear span depth ratio a/d, increases. The Figure 13 is the plot of ultimate load against the beam deflection. The graph shows decrease in the ultimate force and increase in the deflection of beams, Figure 14, is the plot of ultimate force versus crack width for the beams and from the plot, the force on the beams increases with the increase in the crack width of the beams, and Figure 15, is the graph of effective span to depth ratios relationship for the deep beams.

## 5. Conclusions

There were four reinforced concrete deep beam specimens tested in this research, using the shear-span-to-depth ratio and effective span -to- depth ratio as variables to determine their effect on the strength and serviceability limit states. This study can be concluded to yield the following:

The cracking behavior and failure mode of all the deep beams under loading failed by shear–compression failure. This was confirmed by the visual observation of the cracking pattern of the beam specimens, which were influenced by the beam size and the amount of tensile reinforcement.

The experimental results indicate that the ultimate load-carrying capacity increased as the effective span-to-depth ratio ($L_e/h$ ) and shear span-to-depth ratio (a/d) decreased. Beam B4, with the lowest ($L_e/h$ ) ratio of 1.7 and a/d ratio of 0.9, exhibited the highest first crack load (180.79 kN) and ultimate failure load (241.43 kN), while Beam B1, with the highest ratios ($L_e/h = 2.5$, $\frac{a}{d} = 1.4$), recorded the lowest first crack load (89.97 kN) and failure load (124.51 kN). The results demonstrate that reducing the span-to-depth ratio enhances the arching action within deep beams, enabling more efficient transfer of loads directly to the supports and significantly improving structural strength.

Deflection consistently decreased with increasing beam depth and decreasing $L_e/h$ and a/d ratios. The measured deflection reduced from 0.21 mm for Beam B1 to 0.08 mm for Beam B4, representing approximately a 62% reduction. This indicates that deeper beams possess higher flexural stiffness, resulting in improved resistance to deformation under applied loading.

The final crack width increased progressively from 2.54 mm in Beam B1 to 3.58 mm in Beam B4. Although deeper beams developed wider cracks at ultimate failure, they sustained significantly higher loads before reaching failure. The wider crack widths are attributable to the higher stress levels and greater ultimate load capacity achieved before collapse, rather than poor structural performance.

The results reveal an inverse relationship between beam strength and crack width. Beams with greater load-carrying capacity exhibited lower deflections but larger crack widths at failure. Therefore, increasing beam depth improves structural strength and stiffness but may require additional crack-control measures if serviceability requirements are critical.

### *Recommendations*

- For structures where high load-carrying capacity is required, deep beams with lower effective span-to-depth ($L_e/h$)and shear span-to-depth (a/d) ratios are recommended because they provide superior strength and stiffness.
- Although deeper beams achieved higher ultimate loads, they developed wider cracks at failure. Adequate reinforcement detailing, improved reinforcement distribution, or additional crack-control reinforcement should therefore be considered where crack width is an important serviceability criterion.
- Designers should optimize beam depth to achieve a balance between structural strength, stiffness, economy, and crack control rather than focusing solely on increasing ultimate load capacity.
- Further research should investigate the influence of reinforcement ratio, concrete compressive strength, stirrup spacing, and loading conditions on the behavior of deep beams with varying $L_e/h$)and a/d ratios.
- Finite element modelling and analytical strut-and-tie models are recommended to validate the experimental findings and extend the investigation to other beam geometries and loading conditions.
- Future studies should evaluate crack width and deflection under service loads in addition to ultimate loads to provide a more comprehensive understanding of the practical performance of deep beams.

## Compliance with ethical standards

### *Acknowledgments*

We acknowledge Federal University of Technology Akure, Nigeria, and Elizade University, Ilara-Mokin, Ondo State, Nigeria, for granting us access to their Civil Engineering Department Structural Laboratories.

### *Disclosure of conflict of interest*

No conflict of interest to be disclosed.

### *Statement of informed consent*

Informed consent was obtained from all individual participants included in the study.

## References

[1] Sangeeth, S. (2021). Numerical Analysis of Crack Concentration and Propagation in Reinforced Concrete Deep Beams with Varrying Attributes; *International Journal of Innovation in Engineering Research and Technology (IJIERT), 8(6): 11-15.*

[2] Hanoon, A. N., Jaafar, M. S., Hejazi, F. and Aziz, F. N. A. A. (2016). Strut effectiveness factor for reinforced concrete deep beams under dynamic loading conditions. *Case Studies in Structural Engineering, 6: 84–102.*

[3] Yaarub G. A and Hassan F. H. (2020). A Review of Behavoir of Reinforced Concrete Deep Beams. *Journal of Engineering and Sustainable Development (JEASD). 24(05).*

[4] Fan, S., Zhang, Y. Ma, Y. X. and Tan, K. H. (2022). Strut-and-tie and finite element modelling of unsymmetrically-loaded deep beams. *Structures 36: 805–821.*

[5] Hussein, K. K. and Mazin, D. A. (2023). Concrete Deep Beam with Strut Reinforcement. *Muthanna Journal Engineering and Technology (MJET).4(8).*

[6] Seena, P. and Chandran, A. (2021). Shear Strength of Reinforced Concrete Deep Beam. *Innovations in Civil Engineering, Conference paper Marian Engineering College.*

[7] American Concrete Institute Committee 318 (2008). Building Code Requirements for Structural Concrete (ACI 318-08) and Commentary. American Concrete Institute, Farmington Hills,MI. USA, 2008.

[8] Nagarajan, P. and Pillai, T. M. M. (2008). Analysis and design of simply supported deep beams using strut and tie method, *Advances in Structural Engineering, 11 (5): 491–499*.

[9] Guangnan, Z., Zainab, H. A., Mohammed, S. A., Mohamed, H. M., Sinan, O. S., Mohammed, M. H., Zainab, S. A., and Zaher, M. Y., (2022). Reinforced concrete deep beam shear strength capacity modelling using an integrative bio-

inspired algorithm with an artificial intelligence model. *Journal of Engineering with Computer, 38; DOI: 10.1007/s00366-020-01137-1*

[10] American Association of State Highway and Transportation Officials Load and Resistance Factor Design AASHTOLFRD, 2008.

[11] Birrcher, D., Tuchscherer, R., Huizinga, M., Bayrak, O., Wood, S., and Jirsa, J. (2009): *Strength and Serviceability Design of Reinforced Concrete Deep Beams*. Center for Transportation Research, The University of Texas at Austin.

[12] Praveen, N. and T. M Madhavan Pillai (2008). Analysis and Design of simply supported Deep Beams using strut and tie method, *Department of civil Engineering, National Institute of Technology Calicut India.*

[13] Rašeta, A., Starčev-Ćurčin, A., Malešev, M., Kukaras, D., Radonjanin, V., Šešlija, M., and Žarković, D. (2020). *Experimental testing of reinforced concrete deep beams designed by strut-and-tie method. Applied Sciences, 10(18), 6217. https://doi.org/10.3390/app10186217,*

[14] Abdelwahed, B. S. (2026). Analytical and modeling studies on discontinuity regions in reinforced concrete elements: *Review article. Innovative Infrastructure Solutions, 11, 207. https://doi.org/10.1007/s41062-026-02537.*

[15] Lourenço, M. S., Fernández Ruiz, M., Blaauwendraad, J., Bousias, S., Hoang, L. C., Mata-Falcón, J., Meléndez, C., Mihaylov, B. I., Ferreira, M. P., and Faria, D. V. (2023). Design and assessment of concrete structures with strut-and-tie models and stress fields: From simple calculations to detailed numerical analysis. *Structural Concrete, 24(3), 3760–3778. https://doi.org/10.1002/suco.202200647.*

[16] Oguntoye, S.O., Olanitori, L. M., Akingbonmire S.L, and Egbele, W.E. (2026). Evaluation of sand characterization (XRF/XRD/TGA) on the structural performance and thermal stability of deep beams*. International Journal of Science and Research Archive, 2026, 19(01), 1008-1021.*

[17] Mabood, T. (2026). Optimization of Reinforced Concrete Deep Beams Using Data-Driven Parametric Performance Indicators. *Emirati Journal of Civil Engineering and Applications, 4(1),101-117*

[18] Sanal, I. (2020). Effect of shear span-to-depth ratio on mechanical performance and cracking behavior of high strength steel fiber-reinforced concrete beams without conventional reinforcement. *Mechanics of Advanced Materials and Structures, 27(21), 1849–1864.* https://doi.org/10.1080/15376494.2018.1527963]

[19] Engelsmann, S., Peters, S., Spalding, V. and Forstlechner, F. (2014). Designing structures with structural concrete. *Modern Concrete Construction Manual, 70-105.*

[20] Blikharskyy, Y., Selejdak, J., Vashkevych, R., Kopiika, N., and Blikharskyy, Y. (2023) Strengthening Reinforced Concrete eccentrically loaded columns by Concrete Fibre Reinforced Polymer at different levels of initial load. *Engineering Structures 280(5):115694*.

[21] Jian, C., Hang, H., and Yanchao, S. (2017). Discussion on the suitability of concrete constitutive models for high-rate response predictions of RC structures. *International Journal of Impact Engineering, 106: 202 – 216.*

[22] Guo, Y. (2021). Analysis on Concrete Construction Technology in Civil Engineering Construction. *Journal of Physics, doi:10.1088/1742-6596/2011/1/012023.*

[23] Guo, Z. (2014). Basic Mechanical Behavior. Principle of Reinforced Concrete. 9-52. DOI:10.1016/B978-0-12-800859-1.00002-5.

[24] Abtan, Y. and Hassan, F. (2020). A review of behavior of reinforced concrete deep beams. Journal of Engineering and Sustainable Development, 24(05).

[25] Kadhim, H. K., and Abdullah, M. D. (2022). Effect of loading type in concrete deep beam with strut reinforcement. *Open Engineering, 14: 20220488*(2024).

[26] Harsha, G. S. and Raju, P. P. (2019). Shear Strength of Deep Beams: A State of Art*. International Journal of Recent Technology and Engineering (IJRTE), 7(6C2); 2277-3878.*

[27] Abbood, I. S. (2023). Strut-and-tie model and its applications in reinforced concrete deep beams: A comprehensive review. *Case Studies in Construction Materials, 19, e02643. https://doi.org/10.1016/j.cscm.2023.e02643.*

[28] Singh, S. and Sharma, S. (2018). Concrete Mix Design Methods, Verification Study. International *Journal of Advance Research in Science and Engineering, 7(2): 554 – 560.*

[29] Hu, G., Lei, Z., Buqing, C., Shuai, T. (2025). Experimental and theoretical investigation on cracking behavior and influencing factors of steel-reinforced concrete deep beams. *Buildings, 15(11):1812. MDPI. DOI:10.3390/buildings15111812*

[30] Augustino, D.S., Kabubo, C., Kanali, C., and Onchiri, R. O (2022). The orientation effect of opening and internal strengthening on shear performance of deep concrete beam using recycled tyre steel fibres. *Results in Engineering Volume 15, 100561. https://doi.org/10.1016/j.rineng.2022.100561.*